

# Environment-Sensitive Fluorescent Probe for the Human Ether-a-go-go-Related Gene Potassium Channel

Zhenzhen Liu,<sup>†</sup> Tianyu Jiang,<sup>†</sup> Beilei Wang,<sup>†</sup> Bowen Ke,<sup>‡</sup> Yubin Zhou,<sup>§</sup> Lupei Du,<sup>\*,†</sup> and Minyong Li<sup>\*,†</sup>

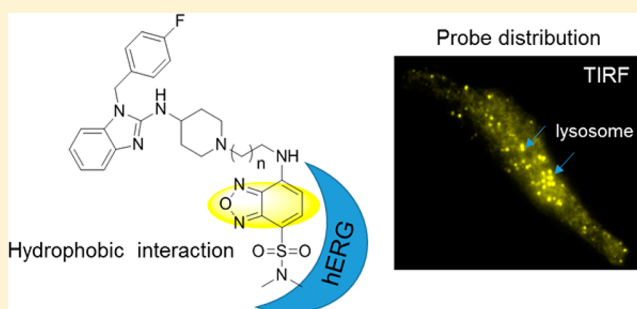
<sup>†</sup>Department of Medicinal Chemistry, Key Laboratory of Chemical Biology (MOE), School of Pharmacy, Shandong University, Jinan, Shandong 250012, China

<sup>‡</sup>Laboratory of Anaesthesiology and Critical Care Medicine, West China Hospital, Sichuan University, Chengdu, Sichuan 610041, China

<sup>§</sup>Institute of Biosciences and Technology, Texas A&M University Health Science Center, Houston, Texas 77030, United States

## S Supporting Information

**ABSTRACT:** A novel environment-sensitive probe S2 with turn-on switch for Human Ether-a-go-go-Related Gene (hERG) potassium channel was developed herein. After careful evaluation, this fluorescent probe showed high binding affinity with hERG potassium channel with an  $IC_{50}$  value of 41.65 nM and can be well applied to hERG channel imaging or cellular distribution study for hERG channel blockers. Compared with other imaging techniques, such as immunofluorescence and fluorescent protein-based approaches, this method is convenient and affordable, especially since a washing procedure is not needed. Meanwhile, this environment-sensitive turn-on design strategy may provide a good example for the probe development for these targets that have no reactive or catalytic activity.



For humans, the information seen by our naked eyes could be trusted. In fact, most things in organisms do not have a signal to be visualized. Therefore, a lot of labeling techniques have been developed, including radioisotopes, fluorescent probes, dye staining, bioluminescence, and chemiluminescence. Currently, these techniques are useful tools to study the physiological process, and each has its advantage. Thus, because of their unique properties, such as high sensitivity and flexibility and convenient operation, small molecule fluorescent probes have a wide range of applications, such as using bioorthogonal reactions to label protein,<sup>1</sup> directly detecting and imaging enzyme, receptor, ion channel, DNA, RNA, bioactive small molecules ( $H_2S$ ,  $H_2O_2$ , etc.), or others,<sup>2–5</sup> and tracing the dynamic process at the cell or animal level. Especially, a near-infrared probe was used to guide surgery in a clinical application.<sup>6,7</sup>

Human Ether-a-go-go-Related Gene (hERG) potassium channel, the rapid component of the delayed rectified potassium channel, is highly associated with drug-induced arrhythmias.<sup>8</sup> To well analyze the hERG channel, a small-molecule fluorescent probe may be a powerful tool, which can provide the real-time information in living systems, and also minimally influence the native properties of the hERG channel. Currently, several types of small molecule fluorescent probes for the hERG channel were reported,<sup>9</sup> including potential sensitive probes (DiSBAC4(3), DiSBAC2(3), CC2-DMPE/DiSBAC2(3), CC2-DMPE/DiSBAC4(3), FMP dye) and  $TI^+$  and  $K^+$  sensitive probes. These probes have been well applied in

hERG channel inhibitor screening. However, the selectivity of these probes for the hERG channel is rather lower, which limited their further application. Therefore, developing selective fluorescent probes for the hERG potassium channel is very meaningful. Now, there are few such probes, and one example is a fluorescent derivative of dofetilide, which is used for the hERG channel inhibitory activity assay based on the fluorescent polarization (FP) method.<sup>10</sup> However, this probe has no off-on fluorescence switch in its structure, which may increase the background signal when imaging. Hence, we subsequently tried our best to develop novel probes with different off-on mechanisms. In our previous work, we have developed two types of small molecule fluorescent probes for the hERG channel based on a PET off-on mechanism,<sup>9,11</sup> which were well applied in cell-based hERG channel inhibitors screening and hERG channel imaging. In this article, we hope to introduce another novel off-on mechanism in the structure, further improve the activity of the probes, and also explore their promising application thereof.

As we know, unlike enzymes and active small molecules that can utilize their catalytic or reactive activity to design a turn-on switch, for those targets with no reactive or catalytic activity, introducing a fluorescent turn-on switch is challenging. Now, it is well studied that a hydrophobic interaction between the

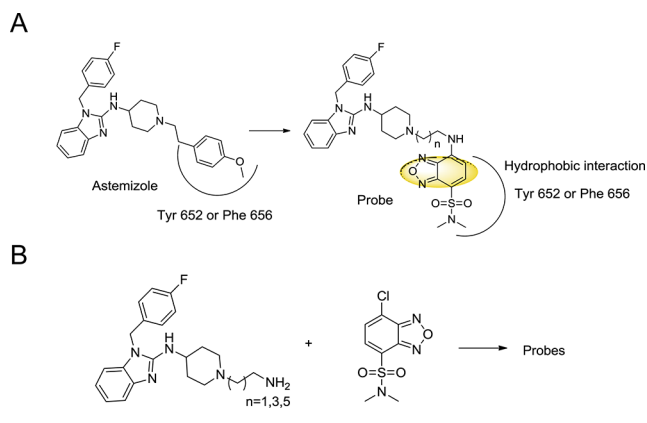
Received: November 6, 2015

Accepted: January 5, 2016

Published: January 5, 2016

ligands and the Tyr 652 or Phe 656 residue of hERG channel plays a critical role for the high binding affinity.<sup>8</sup> Therefore, we can speculate whether we can utilize an environment-sensitive fluorophore to sense this hydrophobic interaction. In fact, this solvatochromic off–on mechanism has already been explored to detect protein conformation dynamics, protein–protein interaction, and structural characterization of the ligand-binding domain,<sup>12–14</sup> which was realized by incorporating a fluorescent environment-sensitive synthetic amino acid to the peptide or protein. In addition, there are several small-molecule fluorescent probes with were reported to detect the hydrophobic pocket based on the environment-sensitive fluorophores, such as 6-dimethylaminonaphthalene (DAN) derivatives, 1,8-anilino-naphthalenesulfonic acid (ANS), and 4-sulfamoyl-7-aminobenzoxadiazole (SBD).<sup>15–18</sup> Inspired by these proof-of-concept results, herein we decided to design an environment-sensitive probe for the hERG channel. In order to obtain a high-affinity probe, Astemizole, the most potent inhibitor of the hERG channel, was chosen as the recognition motif. Considering that small volume fluorophore may minimally influence the binding affinity of the parent ligand, a relative small fluorophore SBD was designed to be incorporated into the structure of Astemizole. In the classical design strategy, the fluorophore was not involved in the binding with the target protein so that the binding activity of the parent ligand was decreased more or less. Therefore, in our design strategy, the fluorophore together with Astemizole was the recognition motif (Scheme 1A). According to the reported

**Scheme 1. (A) Design Strategy of Probes Based on SBD Fluorophore and Astemizole; (B) Synthesis Route of the Probes**



binding mode of Astemizole with the hERG channel, the 4-methoxyphenyl group is involved in the hydrophobic interaction,<sup>19</sup> and therefore, we replaced this group with SBD fluorophore (Scheme 1A) for retaining the hydrophobic interaction.

Subsequently, probes were synthesized through a simple substitution reaction as shown in Scheme 1B. The Astemizole motif and SBD fluorophore were prepared according to the literature (Scheme S1). Afterward, the inhibitory activities of the probes against the hERG channel were evaluated using a radio-ligand competitive binding assay. The experimental result revealed that all probes had high affinities for the hERG channel (Table 1 and Figure S2), and compared with our previous reported probes, the activity was greatly improved. When the length of the linker between the fluorophore and

**Table 1. Fluorescent Properties and hERG Potassium Binding Affinity of Probes S1–S3**

| probe      | <i>n</i> | wavelength (nm) |                 | IC <sub>50</sub> (μM) | K <sub>i</sub> (μM) |
|------------|----------|-----------------|-----------------|-----------------------|---------------------|
|            |          | λ <sub>ex</sub> | λ <sub>em</sub> |                       |                     |
| S1         | 1        | 415             | 581             | 49.69                 | 24.88               |
| S2         | 3        | 435             | 582             | 0.014                 | 0.0069              |
| S3         | 5        | 441             | 579             | 0.16                  | 0.083               |
| Astemizole |          |                 |                 | 0.012                 | 0.0058              |

piperidine ring is four-carbon, the activity is the best with an IC<sub>50</sub> value of 14 nM, which is comparable to Astemizole (12 nM). Meanwhile, a fluorescent polarization assay was also conducted to determine the binding affinity. It was found that the FP value was greatly augmented with the increase of the cell membrane, indicative of an efficient binding (Figure S5). Therefore, in the following experiment, probe S2 was selected for further activity evaluation.

As described above, probe S2 has a high affinity for the hERG channel. However, whether this activity can translate into a functional inhibition of potassium current is not clear. Probe S2 was then tested using the whole-cell voltage patch clamp electrophysiology method on hERG transfected HEK293 cells. As shown in Figure 1, with the increasing concentration of probe S2, the hERG potassium current was decreased, and the calculated IC<sub>50</sub> value is 41.65 nM, which was also comparable to Astemizole.

In our probes, an environment-sensitive fluorophore SBD was introduced to sense the hydrophobic interaction within the hERG channel. To validate this hypothesis, probe S2 was incubated with different concentrations of hERG-transfected HEK293 cell membrane. As illustrated in Figure 2, the fluorescence intensity can be significantly enhanced by the

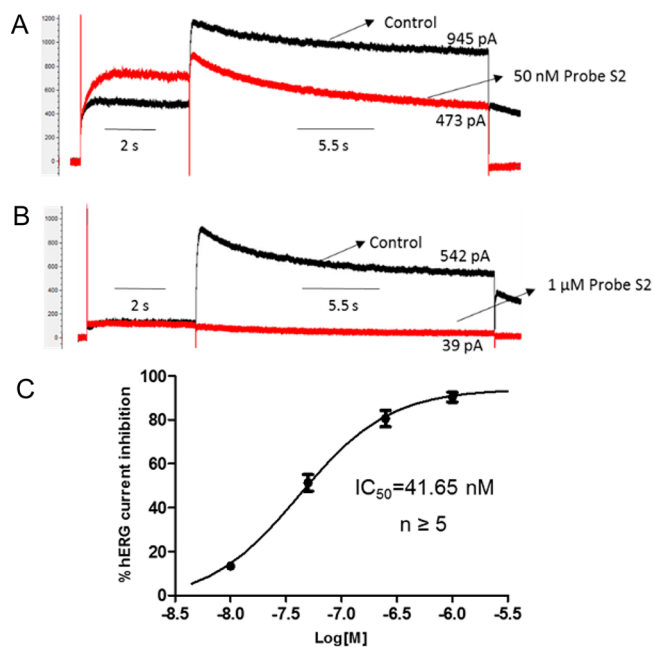


**Figure 1.** Inhibitory activity of probe S2 on hERG determined by the whole-cell voltage patch clamp. (A, B) Examples of the hERG tail current were blocked by probe S2 (50 nM and 1 μM); (C) the percent inhibition of the hERG channel current by different concentrations of probe S2; the IC<sub>50</sub> value was calculated by using the GraphPad Prism 5 software.

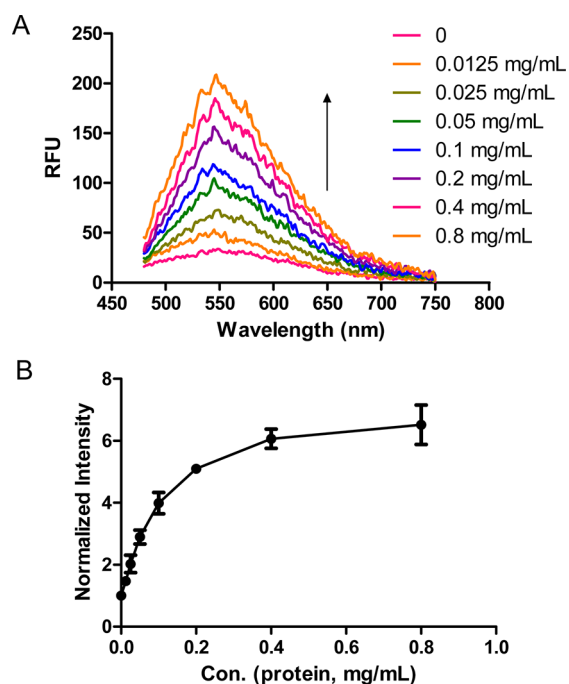


**Figure 2.** (A) Fluorescent emission spectra of  $1 \mu\text{M}$  probe S2 incubated with different concentrations of the membrane for 20 min (excited at 435 nm) and (B) fluorescent intensity (normalized based on the last point that is seen as 1) at 550 nm emission wavelength.

increasing amount of cell membrane. When incubated with 0.8 mg/mL cell membrane, the fluorescence intensity increased about 6-fold compared with the blank control. Meanwhile, the quantum yields of probe S2 also increased about 4-times after binding to 0.0625 mg/mL cell membrane (from 0.0044 to 0.0153, Table S1). Moreover, various concentrations of cell membrane were designed to be incubated with only SBD moiety. Different from probe S2, the fluorescent intensity increase of SBD moiety showed an approximate linear manner and the level of fluorescence enhancement is also lower than that of probe S2 (Figure S3), which indicated that the fluorescence enhancement was not just the result from the nonspecific binding of fluorophore moiety to cell membrane but the specific binding of probe S2 to target protein. In addition, the maximum emission wavelength of probe S2 was blue-shifted about 5 nm from 550 nm in assay buffer (50 mM Tris-HCl, 1 mM MgCl<sub>2</sub>, 10 mM KCl) to 545 nm when membrane was added. The similar environment-sensitive properties were also observed in different polarities of the solvent; fluorescence was higher in a nonpolar solvent and lower in a polar solvent (Figure S1).

Afterward, the selectivity of this fluorescence intensity increase for hERG potassium channel was also explored. In this assay, bovine serum albumin (BSA) and trypsin, which easily form a nonspecific binding with small molecules, were selected as the control group. As shown in Figure 3, probe S2 demonstrated suitable selectivity against BSA and trypsin. However, a certain fluorescence increase and about 5 nm blue shift of the maximum emission wavelength have also been observed for BSA, which indicated that probe S2 may form some nonspecific binding with BSA. In addition, the fluorescence intensity increase of probe S2 induced by incubating with cell membrane can be decreased by Astemizole, a potent hERG channel inhibitor. However, the fluorescence

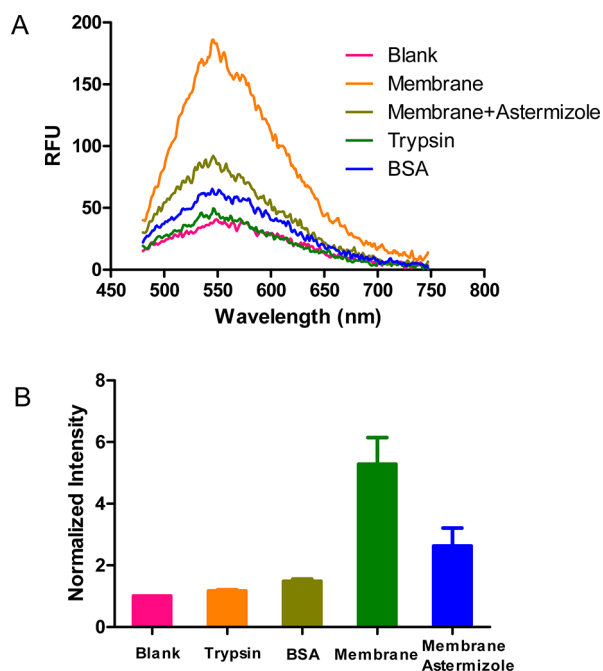


**Figure 3.** Fluorescent emission spectra (excited at 435 nm) and fluorescent intensity changes at the maximum emission wavelength of  $1 \mu\text{M}$  probe S2 incubated with a  $0.5 \text{ mg/mL}$  hERG transfected HEK293 membrane,  $1 \text{ mg/mL}$  trypsin,  $1 \text{ mg/mL}$  BSA, and a  $0.5 \text{ mg/mL}$  hERG transfected HEK293 membrane combined with hERG potassium channel inhibitor Astemizole ( $100 \mu\text{M}$ ) for 20 min.

enhancement could not be completely suppressed, which may be induced by unavoidable nonspecific binding, especially the hydrophobic component.

To further expand the application potential of our probes, we also explored whether probe S2 can be used for hERG channel imaging in living cells. This study was conducted on hERG-transfected HEK293 cells. The fluorescent microscopy results confirmed that the hERG channel can be well selectively labeled, while a significant fluorescence decrease was observed when the cells were coincubated with probe S2 and Astemizole (Figure 4). Notably, a complex washing procedure is not required, which ensures a very convenient imaging process. Considering that the hERG channel is a membrane protein, we also conducted TIRF imaging, and a significant membrane signal can be observed (Figure S6). Interestingly, a lot of light dots in the cytoplasm can be seen, especially in the TIRF imaging. As probe S2 is an alkaline molecule, it may be accumulated in the acidic lysosome as other basic drugs, in which the pH range is 4.5–5. The following costaining experiment confirmed this (Figure S6). The calculated colocalization coefficient of probe S2 with a lysosome blue tracer (synthesized by our lab) is 0.75. Subsequently, chloroquine, a weak base drug that can be accumulated within lysosome and inhibit the intralysosomal trapping of drugs, was used to coincubate with probe S2, and the number of the light dots are also decreased. To exclude the possibility that this lysosome staining is caused by an off-on mechanism based on lysosome acidity, such as PET effect, which was often used as a design strategy for lysosome probe,<sup>20</sup> the fluorescent emission spectra was measured in Britton-Robinson buffer at different pH values. The result demonstrated that there is almost no fluorescence changes with decreasing pH value (Figure S4). Therefore, the specific lysosome staining may be mainly due to

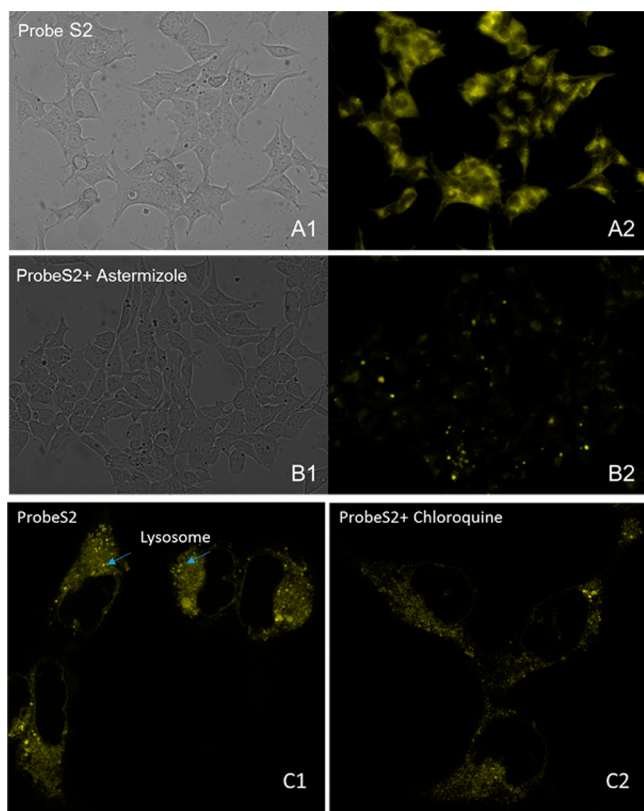


**Figure 4.** (A, B) Fluorescence microscopic imaging of hERG transfected HEK293 incubated with 5  $\mu\text{M}$  probe S2 ((A1) bright field; (A2) green channel) and coincubated with 5  $\mu\text{M}$  probe S2 and 200  $\mu\text{M}$  Astemizole (a potent hERG blocker; (B1) bright field; (B2) green channel). Objective lens: 40 $\times$ . (C) Fluorescent microscopic imaging of hERG transfected HEK293 incubated with 5  $\mu\text{M}$  probe S2 in the absence or presence of chloroquine. Objective lens: 63 $\times$ .

the accumulation of probe S2 in the lysosome, which resulted in the concentration of probe S2 in lysosome being very high, and then, lysosome was stained. This drug accumulation phenomenon is also observed for ABL1 tyrosine-kinase inhibitors (imatinib and nilotinib) using a quantitative hyperspectral stimulated Raman scattering technique, in which drugs were enriched over 1000-fold in lysosomes.<sup>21</sup> This is similar to the results obtained from H3-labeled Astemizole.<sup>22</sup> Therefore, to a degree, the distribution of probe S2 reflected the distribution of Astemizole in cells, and this result may give us some hint that we may design a probe through incorporating a fluorophore to the ligand structure and then use it to explore the pharmacokinetics of the drug with a similar scaffold.

In conclusion, we developed a high-affinity environment-sensitive probe S2, which can be applied for hERG channel imaging with low background signal. Compared with our previous reported probes, the inhibitory activity was greatly improved from micromolar to nanomolar level. Meanwhile, compared with other imaging techniques, such as immunofluorescence and fluorescent protein-based approaches, this method is convenient and affordable, especially since a washing procedure is not needed due to the environment-sensitive switch in the structure. These turn-on design strategies may provide good examples for the probe development for these targets that have no reactive or catalytic activity. In addition, we also found that probe S2 may be used to trace the distribution

of Astemizole in live cells. In fact, there have already been several probes reported, which were used to study the relationship between the chemical structure and subcellular location, the cellular distribution of drugs, and the distribution of the drugs in vivo.<sup>23–25</sup> Therefore, our probe may have a promising application in a hERG channel associated study in the future. However, there are still more efforts to be undertaken, especially in the development of a near-infrared probe for the hERG channel, which may be applied in vivo study.

## ■ ASSOCIATED CONTENT

### 📄 Supporting Information

The Supporting Information is available free of charge on the ACS Publications website at DOI: 10.1021/acs.analchem.5b04220.

NMR spectra, HRMS and experimental details. (PDF)

## ■ AUTHOR INFORMATION

### Corresponding Authors

\*Tel./Fax: +86-531-8838-2006. E-mail: [dulupei@sdu.edu.cn](mailto:dulupei@sdu.edu.cn).

\*Tel./Fax: +86-531-8838-2076. E-mail: [mli@sdu.edu.cn](mailto:mli@sdu.edu.cn).

### Notes

The authors declare no competing financial interest.

## ■ ACKNOWLEDGMENTS

The present project was supported by grants from the National Natural Science Foundation of China (No. 30901836), the Doctoral Fund of Shandong Province (No. BS2012YY008), the China–Australia Centre for Health Sciences Research (CACHSR) (No. 2015GJ02), and the National Institutes of Health (No. RO1GM112003). We also thank Professor Gui-Rong Li from the University of Hong Kong for his generous gift, the hERG-transfected HEK293 cell. Our cell imaging work was performed at the Microscopy Characterization Facility, Shandong University.

## ■ REFERENCES

- (1) Takaoka, Y.; Ojida, A.; Hamachi, I. *Angew. Chem., Int. Ed.* **2013**, *52*, 4088–4106.
- (2) Chan, J.; Dodani, S. C.; Chang, C. J. *Nat. Chem.* **2012**, *4*, 973–984.
- (3) Chen, X.; Tian, X.; Shin, I.; Yoon, J. *Chem. Soc. Rev.* **2011**, *40*, 4783–4804.
- (4) Giepmans, B. N.; Adams, S. R.; Ellisman, M. H.; Tsien, R. Y. *Science* **2006**, *312*, 217–224.
- (5) Lin, V. S.; Chang, C. J. *Curr. Opin. Chem. Biol.* **2012**, *16*, 595–601.
- (6) Keereweer, S.; Kerrebijn, J. D.; van Driel, P. B.; Xie, B.; Kaijzel, E. L.; Snoeks, T. J.; Que, I.; Hutteman, M.; van der Vorst, J. R.; Mieog, J. S.; Vahrmeijer, A. L.; van de Velde, C. J.; Baatenburg de Jong, R. J.; Lowik, C. W. *Mol. Imaging Biol.* **2011**, *13*, 199–207.
- (7) Choi, H. S.; Gibbs, S. L.; Lee, J. H.; Kim, S. H.; Ashitate, Y.; Liu, F.; Hyun, H.; Park, G.; Xie, Y.; Bae, S.; Henary, M.; Frangioni, J. V. *Nat. Biotechnol.* **2013**, *31*, 148–153.
- (8) Sanguinetti, M. C.; Tristani-Firouzi, M. *Nature* **2006**, *440*, 463–469.
- (9) Liu, Z.; Zhou, Y.; Du, L.; Li, M. *Analyst* **2015**, *140*, 8101–8108.
- (10) Singleton, D. H.; Boyd, H.; Steidl-Nichols, J. V.; Deacon, M.; de Groot, M. J.; Price, D.; Nettleton, D. O.; Wallace, N. K.; Troutman, M. D.; Williams, C.; Boyd, J. G. *J. Med. Chem.* **2007**, *50*, 2931–2941.
- (11) Liu, Z.; Wang, B.; Ma, Z.; Zhou, Y.; Du, L.; Li, M. *Anal. Chem.* **2015**, *87*, 2550–2554.

- (12) Cohen, B. E.; McAnaney, T. B.; Park, E. S.; Jan, Y. N.; Boxer, S. G.; Jan, L. Y. *Science* **2002**, *296*, 1700–1703.
- (13) Loving, G.; Imperiali, B. *J. Am. Chem. Soc.* **2008**, *130*, 13630–13638.
- (14) Touthkine, A.; Kraynov, V.; Hahn, K. *J. Am. Chem. Soc.* **2003**, *125*, 4132–4145.
- (15) Kilpin, K. J.; Clavel, C. M.; Edefe, F.; Dyson, P. J. *Organometallics* **2012**, *31*, 7031–7039.
- (16) Koivunen, J. T.; Nissinen, L.; Kapyla, J.; Jokinen, J.; Pihlavisto, M.; Marjamaki, A.; Heino, J.; Huuskonen, J.; Pentikainen, O. T. *J. Am. Chem. Soc.* **2011**, *133*, 14558–14561.
- (17) Zhuang, Y. D.; Chiang, P. Y.; Wang, C. W.; Tan, K. T. *Angew. Chem., Int. Ed.* **2013**, *52*, 8124–8128.
- (18) Liu, Z.; Miao, Z.; Li, J.; Fang, K.; Zhuang, C.; Du, L.; Sheng, C.; Li, M. *Chem. Biol. Drug Des.* **2015**, *85*, 411–417.
- (19) Du, L. P.; Tsai, K. C.; Li, M. Y.; You, Q. D.; Xia, L. *Bioorg. Med. Chem. Lett.* **2004**, *14*, 4771–4777.
- (20) Chen, L.; Li, J.; Liu, Z.; Ma, Z.; Zhang, W.; Du, L.; Xu, W.; Fang, H.; Li, M. *RSC Adv.* **2013**, *3*, 13412.
- (21) Fu, D.; Zhou, J.; Zhu, W. S.; Manley, P. W.; Wang, Y. K.; Hood, T.; Wylie, A.; Xie, X. S. *Nat. Chem.* **2014**, *6*, 614–622.
- (22) Waterkeyn, C.; Laduron, P.; Meuldermans, W.; Trouet, A.; Schneider, Y. J. *Biochem. Pharmacol.* **1987**, *36*, 4129–4136.
- (23) Giedt, R. J.; Sprachman, M. M.; Yang, K. S.; Weissleder, R. *Bioconjugate Chem.* **2014**, *25*, 2081–2085.
- (24) Rosania, G. R.; Shedden, K.; Zheng, N.; Zhang, X. *J. Cheminf.* **2013**, *5*, 44.
- (25) Turner, D. C.; Brand, L. *Biochemistry* **1968**, *7*, 3381–3390.